


Anorthositic lunar regolith breccia Dhofar 1769—Clear indications for repeated mixing of impact melt lithologies

Addi BISCHOFF ^{1*}, Mike KOMNIK^{1,2}, Jakob STORZ¹, and Jasper BERNDT³

¹Institut für Planetologie, University of Münster, Münster, Germany

²Institut für Geologie und Paläontologie, University of Münster, Münster, Germany

³Institut für Mineralogie, University of Münster, Münster, Germany

*Correspondence

Addi Bischoff, Institut für Planetologie, University of Münster, Wilhelm-Klemm-Str. 10, Münster D-48149, Germany.

Email: bischoa@uni-muenster.de

(Received 14 February 2023; revision accepted 28 June 2023)

Abstract—The lunar regolith breccia Dhofar 1769, which was found in 2012 as a single 125 g piece in the Zufar desert area of Oman, contains a relatively large, dark-colored impact melt breccia embedded in a fine-grained clastic matrix. The internal texture of the fragment indicates the repeated melt breccia formation on the lunar surface, their repeated brecciation, and mixing in second, third, and fourth generations of brecciated rock types. The chemical and mineralogical data reveal the incorporation of a feldspar-rich subophitic crystalline melt within a feldspar-rich microporphyratic crystalline melt breccia. This lithic paragenesis itself is embedded within a mafic, crystalline melt breccia. The entire breccia with the three different impact melts has been finally incorporated into the whole rock breccia. The three impact melts are mixtures of different source rocks and impact projectiles, based on the obtained minor and trace element compositions (in particular of Ni and the rare earth elements [REE]) of the impact melt lithologies. For all processes of impact melt formation, additional steps of their brecciation and re-lithification require a minimum number of seven impact processes.

INTRODUCTION

The total mass of the about 600 lunar meteorites found up until 2023 (The Meteoritical Bulletin, 2023) is about three times greater than all lunar samples returned by the Apollo and Luna missions (<385 kg; Korotev, 2023). In total, the lunar meteorites much better represent the lunar surface rocks, as they were ejected from different random sites of the Moon, while the Apollo and Luna samples were collected only from a very small area of the Moon. Still, both sources of lunar materials (from space missions and meteorites) have a very common characteristic: They all have abundant impact melt lithologies as clasts within the breccias formed at the surface.

Dhofar 1769 was found in 2012 as a single 125 g piece in the Zufar desert area of Oman (Bouvier et al., 2017). Based on the classification of the bulk rock published in the Meteoritical Bulletin (MetBull; Bouvier et al., 2017), Dhofar 1769 is an anorthositic highland

breccia with abundant clasts up to 1 cm in size, which are mainly anorthositic lithologies and crystalline impact melt breccias (IMBs). The rock also contains glassy fragments, some of which are highly vesicular, veins, and impact spherules (mostly devitrified) embedded in a fine-grained clastic matrix (Bouvier et al., 2017). The spherules within the fine-grained matrix indicate an origin at the lunar surface. As accessory minerals, occurrences of ilmenite, troilite, FeNi metal, and zircon have been reported (Bouvier et al., 2017).

First analyses published in the Meteoritical Bulletin (Bouvier et al., 2017) have shown that plagioclase in the bulk rock is anorthitic in composition with a mean of $An_{93.4\pm 5.1}$ (total range: An_{70-97} ; $n = 32$). Olivine is highly variable ranging from 20 to 60 mole% Fa (mean: $Fo_{40\pm 9}$; $n = 16$). The low-Ca pyroxene also shows variable composition with $Fs_{20-58}En_{29-77}Wo_{2.5-15}$ (mean: $Fs_{37.5\pm 10}En_{54.6\pm 10}Wo_{7.8\pm 3.3}$; $n = 28$). Some analyzed Ca pyroxenes have a variable composition of $Fs_{18-34}En_{28-45}Wo_{33-41}$ (Bouvier et al., 2017).

Crystalline IMBs are characteristic lithologies in all kinds of lunar rocks. Based on the mineralogy and texture, Stöffler et al. (1980) defined different types of IMBs, which are very abundant in fragmental feldspathic breccias of Station 11 and Station 13 from Apollo 16 (Stöffler et al., 1981, 1985). Feldspathic fragmental breccias from these stations contain up to 94 area% of IMBs in the size range of 0.05–4 mm (Stöffler et al., 1985). Studies of the clast population statistics of lunar meteorites have also shown that IMBs belong to the most abundant clast types (e.g., Bischoff et al., 1987, 1998; Ostertag et al., 1986; Ryder & Ostertag, 1983).

However, whereas some data on the impact melt lithologies from Apollo samples (or their rare earth element [REE] patterns) have been published (e.g., Korotev, 1994, 1996; Stöffler et al., 1985), very few studies of trace elements in melt rock clasts in lunar meteorites have been reported (e.g., Joy et al., 2010).

Within a thin section from lunar meteorite Dhofar 1769, a conspicuous fragment was found that is obviously a large, several millimeter-sized IMB (Figure 1 and Figure S1). The internal texture of the fragment motivated this study, which is aimed at revealing detailed information about the repeated formation of impact melts on the lunar surface.

SAMPLE AND ANALYTICAL METHODS

The polished thin section (PTS) of Dhofar 1769 (PL15019) from the Institut für Planetologie (Münster) was studied by optical and electron optical microscopy. A ZEISS polarizing microscope (Axiophot) was used for optical microscopy in transmitted and reflected light. A JEOL 6610-LV electron microscope (SEM) at the Institut für Planetologie of the University of Münster was used to study the fine-grained textures and to identify the different mineral phases.

Most quantitative mineral analyses were obtained by new microprobe analyses using the JEOL JXA 8530F electron microprobe (EPMA) at the Institut für Mineralogie in Münster, which was operated at 15 kV and a probe current of 15 nA. Natural and synthetic standards were used for wavelength-dispersive spectrometry (WDS). Jadeite (Na), kyanite (Al), sanidine (K), chromium oxide (Cr), San Carlos olivine (Mg), hypersthene (Si), diopside (Ca), rhodonite (Mn), rutile (Ti), fayalite (Fe), apatite (P), celestine (S), cobalt metal (Co), and nickel oxide (Ni) were used as standards for mineral analyses. Representative analyses of the major minerals are given in Tables S1a–S1c. The bulk chemical compositions of the major elements were also obtained by EPMA using a defocused electron beam of 20 μm . The metal analyses were corrected for Fe/Co interferences.

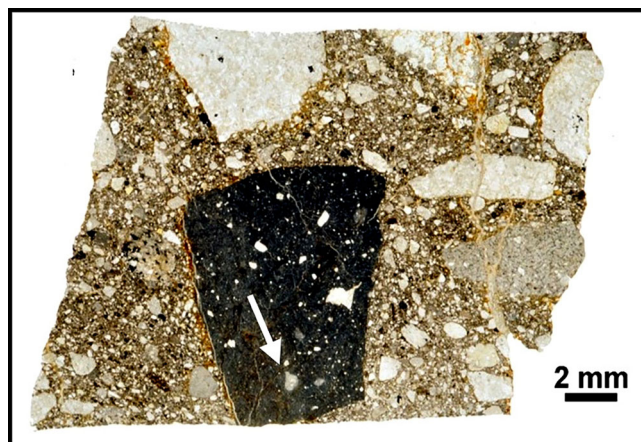


FIGURE 1. Thin section Dhofar 1769 (PL15019) studied at the Institut für Planetologie (Münster). The lunar regolith breccia contains abundant large, light-colored lithic clasts and the dark IMB (which is the IM-3 lithology of the present study) embedded in a fine-grained clastic matrix. Data on the dark IMB with one particular impact melt fragment (arrow; see Figure 2) are discussed in this study. Image in transmitted light. (Color figure can be viewed at wileyonlinelibrary.com)

Using the SEM for quantitative analysis, samples and appropriate mineral standards were measured at an excitation voltage of 20 kV, and the beam current constancy was controlled by a Faraday cup. The attached energy-dispersive X-ray spectroscopy (EDS) system was used for chemical characterization and analyses of the different mineral constituents. Astimex reference materials olivine (Mg, Fe, Si), jadeite (Na), plagioclase (Al), sanidine (K), diopside (Ca), rutile (Ti), chromium-oxide (Cr), rhodonite (Mn), and pentlandite (Ni) were used as natural and synthetic standards. For these EDS analyses, the INCA analytical program provided by Oxford Instruments was used.

The abundances of minor and trace elements of the individual melt lithologies were analyzed on the thin section at the Institut für Mineralogie (Münster) by a ThermoScientific Element XR single-collector inductively coupled plasma mass spectrometer (ICP-MS) coupled with an Excimer laser ablation system (Analyte G2, Photon Machines). The latter provided an output wavelength of 193 nm and was operated with a fluence of 3 J cm^{-2} and a repetition rate of 10 Hz. Counting times were 40 s on peak signals and 20 s on background. The analyses were obtained using variable spot sizes of 25–65 μm . External reference material was NIST-SRM 612 glass. For quantification, ^{29}Si was used as an internal standard. To keep track of precision and accuracy over the course of this study, basaltic BIR-1G (Jochum et al., 2005) and phosphatic STDP5 (Klemme et al., 2008) reference glasses were measured as unknowns.

RESULTS

Mineralogy

The thin section PL15019 is dominated by six larger lithic clasts (each $>5 \text{ mm}^2$) and several smaller ones embedded in a fine-grained clastic matrix (Figure 1). The largest fragment of about 1 cm^2 is the complex IMB and the main object of this investigation. Most other large lithic fragments are metamorphosed anorthositic (gabbroic, noritic) rocks and breccias, which should be classified as granulitic rocks and breccias according to the classification scheme of Stöfler et al. (1980). Besides the well-studied IMB, a second IMB exists that, again based on Stöfler et al. (1980), has to be classified as a crystalline, fine-grained subophitic IMB. The matrix consists of small fragments of all the different millimeter-sized lithologies mentioned above, as well as mineral and melt clasts. The individual clasts within the matrix usually have sizes $<500 \mu\text{m}$. Some porosity between the clasts was noted as well as cracks penetrating throughout matrix and clasts that are typically filled by terrestrial carbonates. The most abundant mineral of the matrix is plagioclase, followed by less-abundant mafic minerals (mainly pyroxenes and olivine). As rare phases, spinels, ilmenites, zircon, and metal grains were detected.

As mentioned above, the largest fragment within the studied PTS is about 1 cm^2 and has a dark appearance in plane-polarized, transmitted light (Figure 1). This fragment is a complex IMB containing abundant light-colored lithic and mineral clasts (Figure 1). One of these lithic clasts within the melt rock clast is an IMB that encloses another melt lithology (Figure 2). Thus, three different melt lithologies are enclosed in each other and are also enclosed by fine-grained clastic matrix of the bulk meteorite breccia. These impact melt lithologies are defined as IM-1, IM-2, and IM-3 (Figure 2).

IM-1 is the innermost impact melt lithology and very rich in anorthitic plagioclase laths up to about $100 \mu\text{m}$ in length (Figure 2b; Komnik, 2021). It has a subophitic texture and has to be defined as a crystalline, feldspar-rich, subophitic IMB after Stöfler et al. (1980). Besides the abundant anorthites, fine-grained olivine and pyroxenes occur within the interstices. Several small ($<3 \mu\text{m}$) Fe,Ni grains were observed within IM-1 (Figure 3) as well as one ilmenite and one sulfide grain (probably troilite). The plagioclase is homogeneous in composition, with a mean of $\text{An}_{96.4}\text{Ab}_{3.4}\text{Or}_{0.2}$ (Figure 4). The small number of analyzed olivine grains reveals a mean of $\text{Fa}_{42.3}$ (Figure 5). The pyroxenes are highly variable in composition. The Ca-rich pyroxene has a mean composition of $\text{Fs}_{23.9\pm 3.4}\text{En}_{47.5\pm 3.8}\text{Wo}_{28.6\pm 7.1}$ ($n = 6$). The two analyzed low-Ca pyroxenes ($\text{Fs}_{28.2}$ and $\text{Fs}_{29.2}$) have a considerable Wo contents of about 17 mole%.

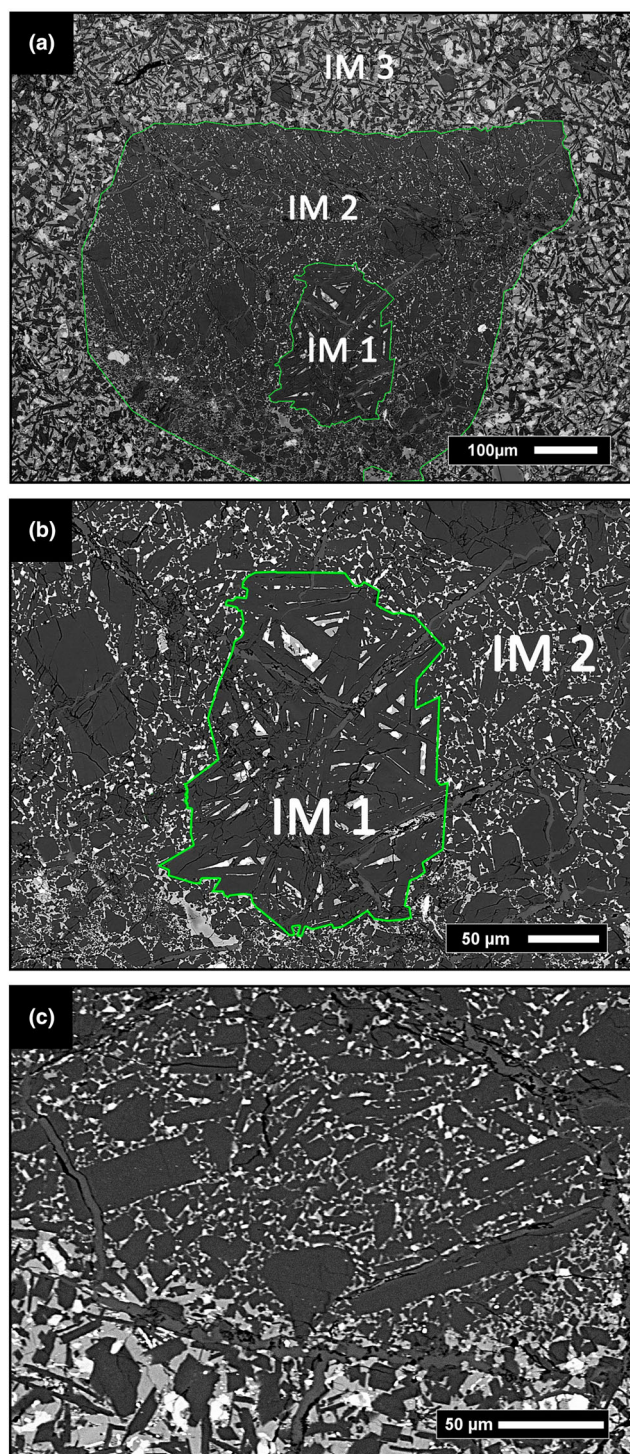


FIGURE 2. (a) The mafic crystalline melt breccia (IM-3) contains another fragment of a feldspar-rich melt breccia (IM-2). (b) IM-2 contains large plagioclase clasts (dark gray) and a crystalline subophitic melt fragment (IM-1) with abundant anorthite laths and interstitial mafic materials (mostly Ca pyroxene and olivine). (c) Boundary between the feldspathic, microporphyrific crystalline melt breccia (IM-2; upper part) and the mafic crystalline melt breccia (IM-3; lower part). Backscattered electron (BSE) images. (Color figure can be viewed at wileyonlinelibrary.com)

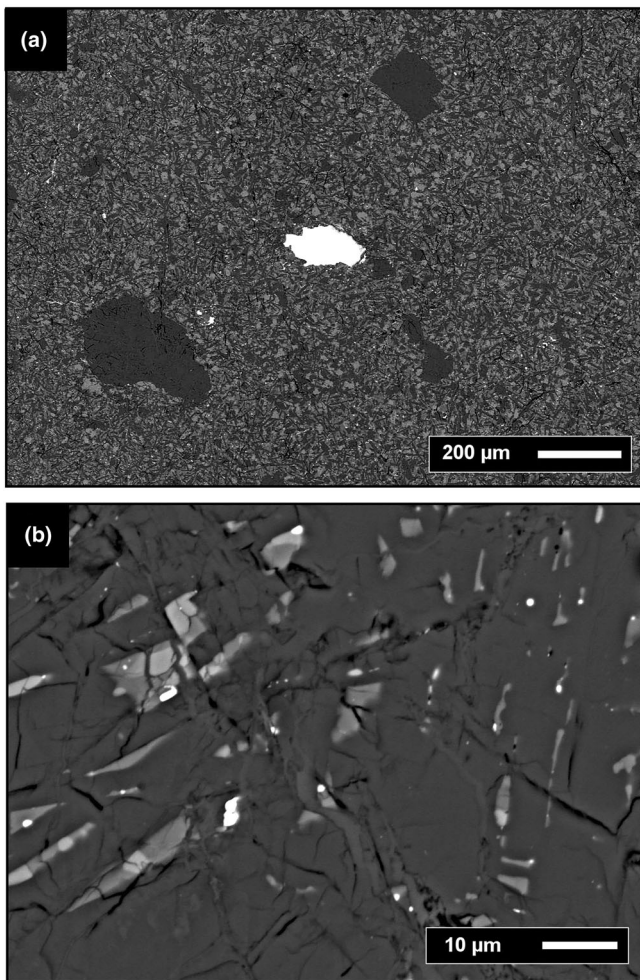


FIGURE 3. Fe,Ni metal grains within the melt lithologies from Dhofar 1769. (a) The largest Fe,Ni metal grain occurs within IM-3. This impact melt has abundant mafic silicates (pyroxenes, olivines; medium gray) and also contains some large anorthite-rich fragments (dark gray). (b) Abundant very small metal grains (white) have been observed in IM-1. They are embedded in silicates: anorthite (dark gray) and mafic silicates (medium gray; light gray); BSE images.

IM-2 encloses IM-1 and has to be classified as a feldspathic, fine-grained to microporphyritic crystalline melt breccia (Stöffler et al., 1980). This lithology is also rich in anorthitic plagioclase (Figure 2a; Komnik, 2021). Besides the impact melt fragment IM-1, some other large plagioclase clasts are embedded within a crystalline fine-grained groundmass of small anorthite laths (typically $< 30 \mu\text{m}$; Figure 2), which are surrounded by mafic phases (mostly olivine and pyroxenes). In addition, small grains of chromite, ilmenite, sulfide, and Fe,Ni metal were observed. The boundary to IM-3 is sharp and well defined (Figure 2c). Like in IM-1, plagioclase is also quite homogeneous in composition with a mean of $\text{An}_{95.7}\text{Ab}_{3.9}\text{Or}_{0.4}$ ($n = 25$; Figure 4). One grain with a significantly lower An content ($\text{An}_{91.8}$) was detected. Ten

olivine grains were analyzed, revealing a mean of $\text{Fa}_{40.1}$ (range: $\text{Fa}_{38.7-43.1}$; Figure 5). The Ca pyroxenes and low-Ca pyroxenes are relatively variable in composition, of $\text{Fs}_{20.4 \pm 3.6}\text{En}_{48.2 \pm 2.2}\text{Wo}_{31.4 \pm 4.6}$ ($n = 16$) and $\text{Fs}_{27.7 \pm 2.2}\text{En}_{61.3 \pm 7.2}\text{Wo}_{11.0 \pm 6.8}$ ($n = 4$), respectively.

IM-3 is rich in mafic minerals (olivine and pyroxenes) filling the large interstices within the fine-grained network of small plagioclase laths (Figure 2; Komnik, 2021). IM-3 certainly represents a mafic crystalline IMB. Besides the above-mentioned light-colored lithic and mineral clasts, IM-3 contains small ilmenite, chromite, sulfide, and Fe, Ni metal grains. Some relatively large-sized metal grains (Figure 3) were observed, as well as areas with several small, partly rounded grains of metal and sulfide. The compositions of metals are given in Table S2. Plagioclase in IM-3 is variable in composition and probably represents plagioclase crystallized from the IM-3 melt, as well as plagioclase crystals that were incorporated as clasts into the impact melt (Figure 4). Therefore, both types can be regarded as separate populations. The crystallized plagioclase from IM-3 has a mean of $\text{An}_{84.9}\text{Ab}_{12.4}\text{Or}_{2.7}$ ($n = 42$; Figure 4), whereas the second (clast) population has a mean of $\text{An}_{95.3}\text{Ab}_{4.2}\text{Or}_{0.5}$ ($n = 16$; Figure 4). Olivine is slightly variable with a mean of $\text{Fa}_{39.9}$ ($n = 33$; Figure 5). As in the other melt lithologies, Ca pyroxenes and low-Ca pyroxenes are variable in composition, with average values of $\text{Fs}_{22.1 \pm 3.3}\text{En}_{47.6 \pm 3.7}\text{Wo}_{30.3 \pm 6.9}$ ($n = 15$) and $\text{Fs}_{34.1 \pm 16.7}\text{En}_{56.4 \pm 14.8}\text{Wo}_{9.5 \pm 6.2}$ ($n = 11$), respectively. Considering the low-Ca pyroxenes, the Fs contents vary significantly between $\text{Fs}_{25.3}$ and $\text{Fs}_{84.1}$.

Bulk Chemistry of the Three Different Impact Melts

The chemical compositions of the three impact melt lithologies (IM-1 to IM-3) are presented in Tables 1 and 2. Considering the major element data, it is obvious that FeO , MgO , and TiO_2 are increasing significantly from IM-1 to IM-3, whereas the CaO and Al_2O_3 concentrations are decreasing (Table 1). This is consistent with the observation mentioned above that the mafic components (olivine, pyroxenes) are more abundant in IM-3 than in IM-1. The minor and trace element concentrations are given in Table 2, and the REE data are also presented in Figure 7. For most elements, the same trends can be observed: The concentrations of minor and trace elements are higher in IM-3 than in IM-1. There are only a few exceptions to this trend. The most significant exception is the high value of Ni in IM-1 compared to the Ni concentration in IM-3. This relationship will be discussed in detail below. Considering the REE data, IM-1 has the lowest element abundances among the impact melt lithologies with a distinct positive Eu anomaly (Figure 7). The REE pattern of IM-2 is

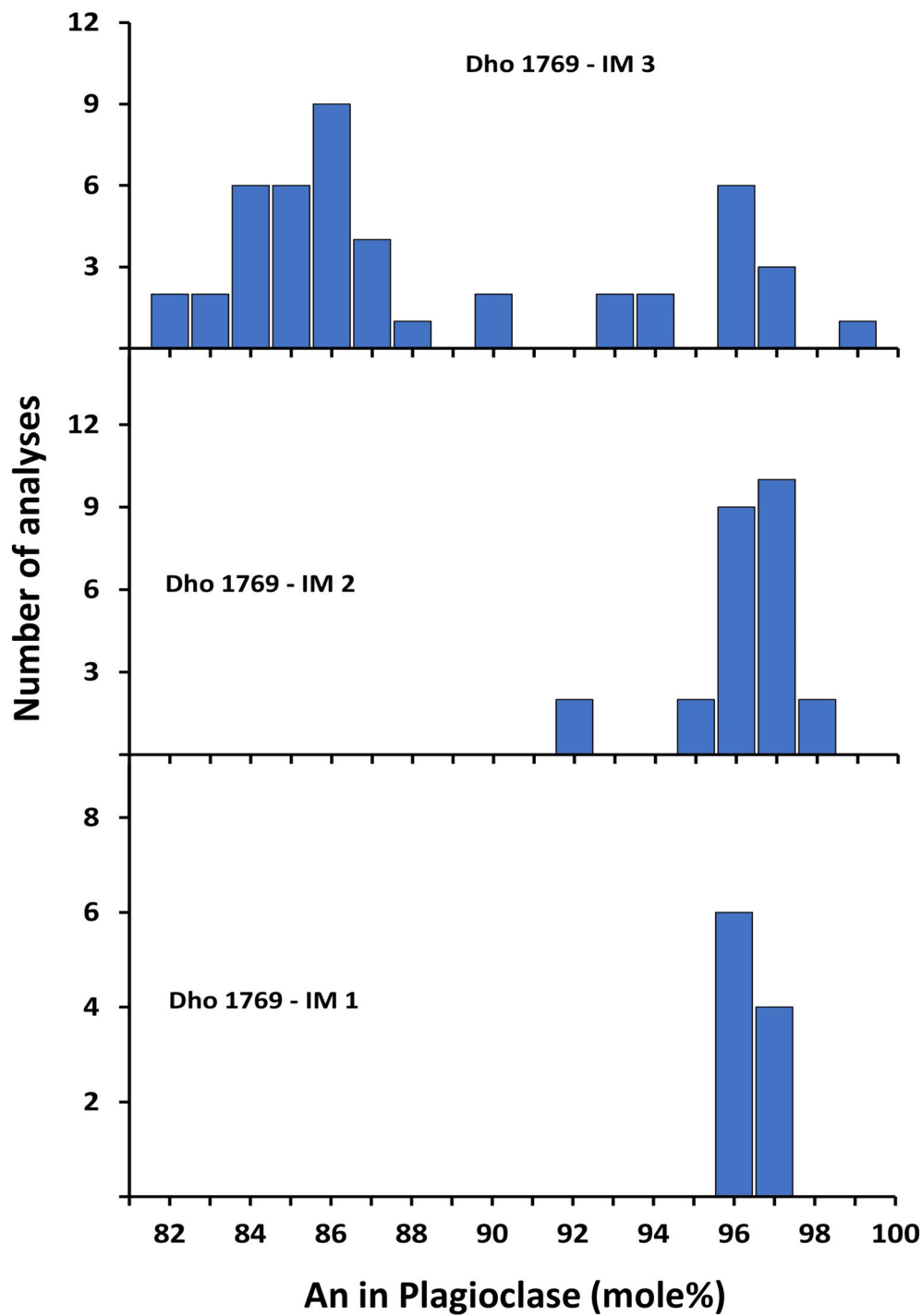


FIGURE 4. Composition of plagioclase within the three impact melt lithologies (IM-1 to IM-3; Komnik, 2021). Plagioclase within the impact melt lithologies IM-1 and IM-2 are very An rich, whereas plagioclase in IM-3 is variable in composition and probably represents plagioclase crystallized from the melt as well as plagioclase grains that were mixed as An-rich clasts into the impact melt. An, anorthite. (Color figure can be viewed at wileyonlinelibrary.com)

relatively flat with an about $20\times$ enrichment compared to CI chondrites (Barrat et al., 2012). IM-3 is about 100 times enriched (relative to CI chondrites) and has a strong negative Eu anomaly (Figure 7). This phase is

similar in composition to the Apollo KREEP basalt 15386 (Warren & Wasson, 1978).

The high Ba and Sr concentrations in the impact melt inclusions of Dho 1769 are most likely due

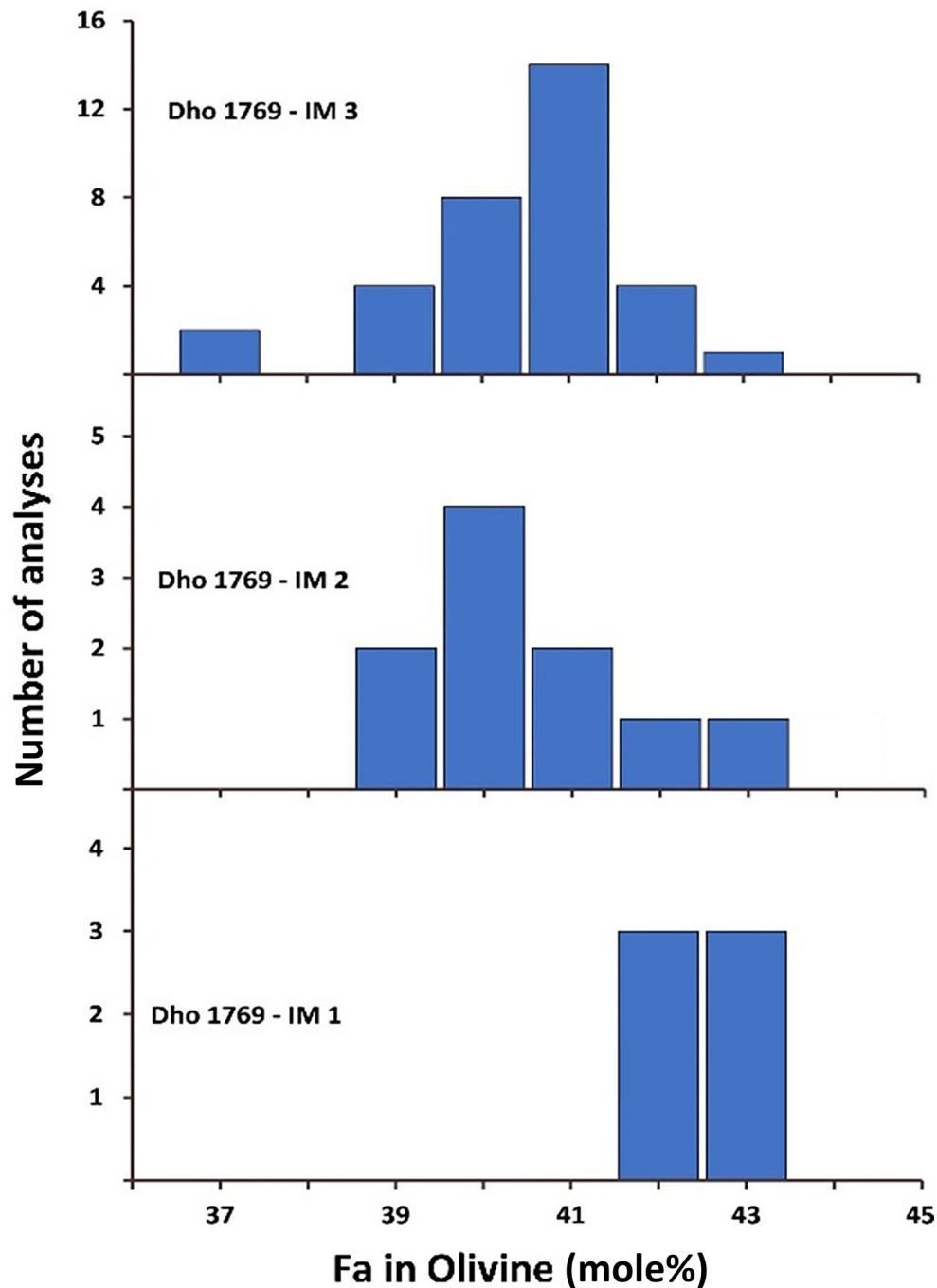


FIGURE 5. The compositions of olivine within the three impact melt lithologies (IM-1 to IM-3; Komnik, 2021). Olivine within IM-1 is very homogeneous in composition, whereas somewhat variable olivine compositions were found in IM-2 and IM-3. Fa, fayalite. (Color figure can be viewed at [wileyonlinelibrary.com](https://onlinelibrary.com))

to a significant contribution by terrestrial alteration, which is also visible by the occurrence of abundant carbonate veins that cross-cut the entire sample. Similar observations were made by Stelzner et al. (1999), who studied the chemical modifications of desert meteorites in dependence of the degree of terrestrial alteration.

DISCUSSION

Abundance of Impact Melt Lithologies in Lunar Surface Rocks

A huge number of millimeter-sized lithic fragments in Apollo regolith samples have been studied in the past,

TABLE 1. Major element bulk chemical compositions of the three impact melt lithologies (IM-1 to IM-3) from Dhofar 1769 obtained by electron microprobe. All elements as oxides.

	IM-1 (<i>n</i> = 70), mean	IM-2 (<i>n</i> = 96), mean	IM-3 (<i>n</i> = 100), mean
SiO ₂	43.17	44.27	46.05
TiO ₂	0.14	0.30	1.56
Al ₂ O ₃	31.20	28.81	18.02
Cr ₂ O ₃	0.06	0.09	0.20
NiO	<0.05	<0.05	<0.05
FeO	2.55	3.76	9.89
MnO	0.04	0.09	0.14
MgO	2.07	3.50	9.46
CaO	18.19	16.91	11.33
Na ₂ O	0.47	0.50	0.69
K ₂ O	0.09	0.14	0.46

and many of these fragments are IMBs (e.g., Jolliff et al., 1991, 1996; Korotev, 1987, 1994, 1996; Stöffler et al., 1985). Impact melt rocks in Apollo samples were intensively studied by Stöffler et al. (1980, 1985), who used mineralogy, texture, and chemical composition to distinguish between “feldspathic” and “mafic” types of crystalline melt breccias. Their data clearly show that crystalline IMBs are characteristic lithologies of lunar surface rocks and are very abundant in fragmental feldspathic breccias of Station 11 and Station 13 from Apollo 16 (Bischoff, Stöffler, et al., 1983; Borchardt et al., 1983; Reimold & Borchardt, 1984; Stöffler et al., 1985). In detail, feldspathic fragmental breccias from these stations contain up to 94 area% of IMBs in the size range of 0.05–4 mm (Stöffler et al., 1985). This is also the case considering most lunar meteorites. Earlier studies on the clast population statistics of the lunar meteorites ALHA81005, Yamato (Y)-791197, Y-82192, Y-82193, Y-86032, MAC 88104, QUE 93069, DaG 282, DaG 400, and Kalahari 008 have shown that all these breccias have more than 15 vol% of crystalline melt breccias (e.g., Bischoff, 1996; Bischoff & Stöffler, 1984, 1985; Bischoff & Weber, 1997; Bischoff et al., 1986, 1987, 1998; Ostertag et al., 1986; Palme et al., 1990, 1991; Sokol & Bischoff, 2005; Sokol et al., 2008; Zipfel et al., 1998). In samples of Y-86032 and MAC 88104, about one half of the registered fragments are crystalline IMBs, and in most cases, the feldspathic melt breccias dominate over the mafic ones (Bischoff et al., 1998). As an example, in QUE 93069, the feldspathic fine-grained to microporphyrific crystalline melt breccias (21.9 vol%) and the feldspathic subophitic crystalline melt breccias (5.2 vol%) are significantly more abundant than the comparatively rare mafic crystalline melt breccias (1.3 vol%; Bischoff, 1996).

TABLE 2. Minor and trace element abundances of the three impact melt lithologies (IM-1 to IM-3) from Dhofar 1769 obtained by laser ablation ICP-MS. All data in ppm.

	IM-1 (<i>n</i> = 9)	IM-2 (<i>n</i> = 35)	IM-3 (<i>n</i> = 59)
Sc	5.8	8.4	30.2
Ti	791	1710	9240
V	13.5	18.3	48
Cr	421	700	1514
Mn	309	431	1159
Co	10.3	8.6	13
Ni	87	38	31
Cu	2.7	3.0	4.0
Ga	3.4	4.4	14
Rb	1.35	1.65	11.5
Sr	462	272	360
Y	5.1	19.5	130
Zr	13	63	565
Nb	1.1	5.1	38.6
Cs	0.76	0.39	0.51
Ba	29	77	497
La	1.5	5.6	41
Ce	4.0	14.4	106
Pr	0.49	1.9	14
Nd	2.4	8.9	64
Sm	0.75	2.6	18
Eu	0.66	0.81	2
Gd	1.23	3.3	21
Tb	0.16	0.55	3.7
Dy	0.99	3.6	24
Ho	0.22	0.77	5.1
Er	0.60	2.2	14.8
Tm	0.09	0.32	2.1
Yb	0.56	2.3	14.1
Lu	0.08	0.32	2.0
Hf	0.38	1.7	14
Ta	0.073	0.23	1.7
W	0.15	0.17	0.7
Pb	0.24	0.72	3.4
Th	0.25	1.1	8
U	0.11	0.30	2

As stated above, IMBs occur as clasts in many lunar meteorites; however, in some cases, entire lunar meteorites can be regarded as IMBs. In the Meteoritical Bulletin Database, these are often classified as melt breccias and are glassy matrix breccias (R. Korotev, pers. comm., 2022; Korotev, 2023). In such cases, the fragments are embedded in a (mostly) glassy, schlieren-rich groundmass formed during impact-induced lithification (e.g., Bischoff et al., 2006; Bischoff, Rubin, et al., 1983; Bischoff & Stöffler, 1992; Kieffer, 1975). An excellent example is the glass-rich, melt matrix breccia Dhofar 081 (Figure 8; Bischoff, 2001). Based on the

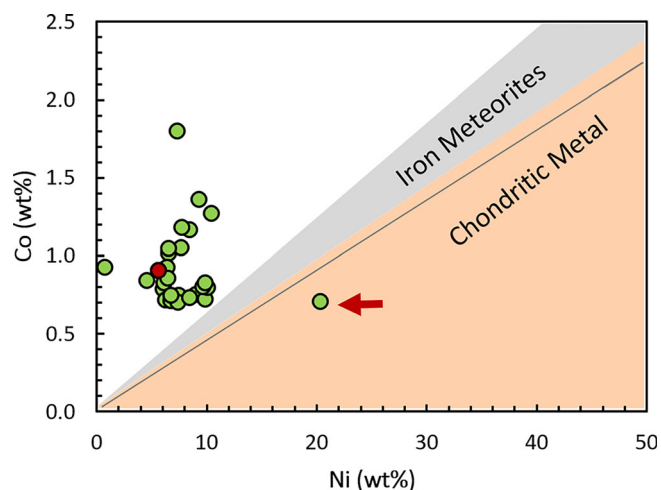


FIGURE 6. Ni/Co ratios of metal grains in the complex impact melt lithology of Dhofar 1769: 26 grains from IM-3 (green) and one grain from IM-2 (red). The metal grains in IM-1 were too small for quantitative analysis without contamination by surrounding phases. The black line corresponds to the chondritic trend. Compositional range of Ni/Co for chondritic metal (orange) and iron meteorites (gray) after Day (2020). Except for one grain (arrow), all analyzed metal grains from the impact melt lithologies are different from those typically characterizing a chondritic or iron meteorite origin. (Color figure can be viewed at wileyonlinelibrary.com)

chemical composition, the bulk rock of Dhofar 081 clearly has a lunar highland bulk composition (Warren et al., 2005; see also Figure 9).

Metals as Indicators of Melt Contamination by Impacting Projectiles?

Considering the metal analyses obtained in the complex impact melt lithologies (Figure 6; data in Table S2), except for three analyses, all data plot in a close range between ~5 and 10 wt% Ni, the abundance typical for kamacite. The three outliers are unusually (1) Ni-poor, and (2) Co-rich or (3) Co-poor. One grain situated in the IM-2 lithology shows a similar Ni/Co ratio as the average Ni/Co ratio of 6.2 for the large number of metal grains within IM-3. The majority of Ni/Co ratios is lower than the average chondritic Ni/Co ratio (~22; Barrat et al., 2012). The individual Ni/Co ratios are difficult to explain and most metals plot outside of the field typical for meteoritic metals (see Figure 6). The redistribution of siderophile elements could be related to impact and might reflect a complex origin that may have included remelting/recrystallization events experienced during shock melting and annealing. This is the only possible scenario we could offer as an explanation. Shock melting and annealing are certainly required as contributing processes in the case of the complex clast

that allowed to clearly identify different impact melt lithologies, and which is, potentially, also a manifestation of multiple melting events. Yet, no metal analysis in the IM-1 lithology was obtained, as the metal grains were smaller than the minimum electron beam diameter of about 3 μm (Figure 3).

Chemical Characteristics of Impact Melt Lithologies IM-1 to IM-3 and Comparison with Melt Breccias in Other Lunar Rocks

Although the occurrence of abundant clasts of IMBs in lunar meteorites is well documented, as mentioned above (e.g., Bischoff et al., 1998; Ostertag et al., 1986; Ryder & Ostertag, 1983), rarely bulk chemical data of individual clasts have been published. Yet, discoveries of large, up to centimeter-sized clasts of melt breccias have been made in the lunar meteorites Sayh al Uhaymir (SaU) 169, MIL 09036, NWA 7022, and NWA 10783, from which at least some preliminary chemical data exist (R. Korotev, pers. comm., 2022).

Lunar meteorite Sayh al Uhaymir 169 includes a large clast of an IMB extremely enriched in potassium, REE (La: ~700 \times CI; Figure 9), and phosphorus (Gnos et al., 2004). This lithology is significantly (~4 \times) enriched in REE compared to the mafic IMB IM-3 (La: ~175 \times CI) and is also enriched in REE relative to KREEP basalt 15386 (La: ~250 \times CI; Figure 7), pointing toward a very KREEPy source.

Preliminary elemental abundances determined by instrumental neutron activation analysis on subsamples of NWA 7022 are as follows (matrix/[melt] clast): 5.2/6.2% FeO, 0.60/0.70% Na₂O, 10.3/13.4 ppm Sc, 200/140 ppm Ni, 5.6/9.1 ppm Sm, 1.36/1.54 ppm Eu, 2.0/3.0 Th (Kuehner et al., 2012; compare Korotev and Irving (2021) for final data). One-third of the NWA 7022 meteorite comprises a single large (up to 4 cm), light-gray, fine-grained (melt) clast (which itself contains small remnant clasts; Korotev, 2023). Korotev (2023) suggested that a sample of NWA 10783 is from a light-colored clast, which he would call a KREEP-bearing, metal-rich, feldspathic IMB on the basis of texture and composition (6.0 wt% FeO, 3.4 ppm Sm, 16 ppb Ir).

Considering data for Apollo KREEP-rich melt breccias of noritic composition from Korotev (2000), IM-3 most closely resembles A15-B and A17-H. Compared to Apollo mafic impact-melt breccias (19–21 ppm Sc), IM-3 is considerably richer in Sc (30 ppm), suggesting that it contains a component of mare basalt.

The REE pattern of IM-3 is also similar to that of the mafic intergranular melt breccia 67075 from Apollo 16 (Stöffler et al., 1985). It is also similar to some other data from samples from Apollo 17 (Figure 9; Jolliff et al., 1996) and for mafic melt breccias published by

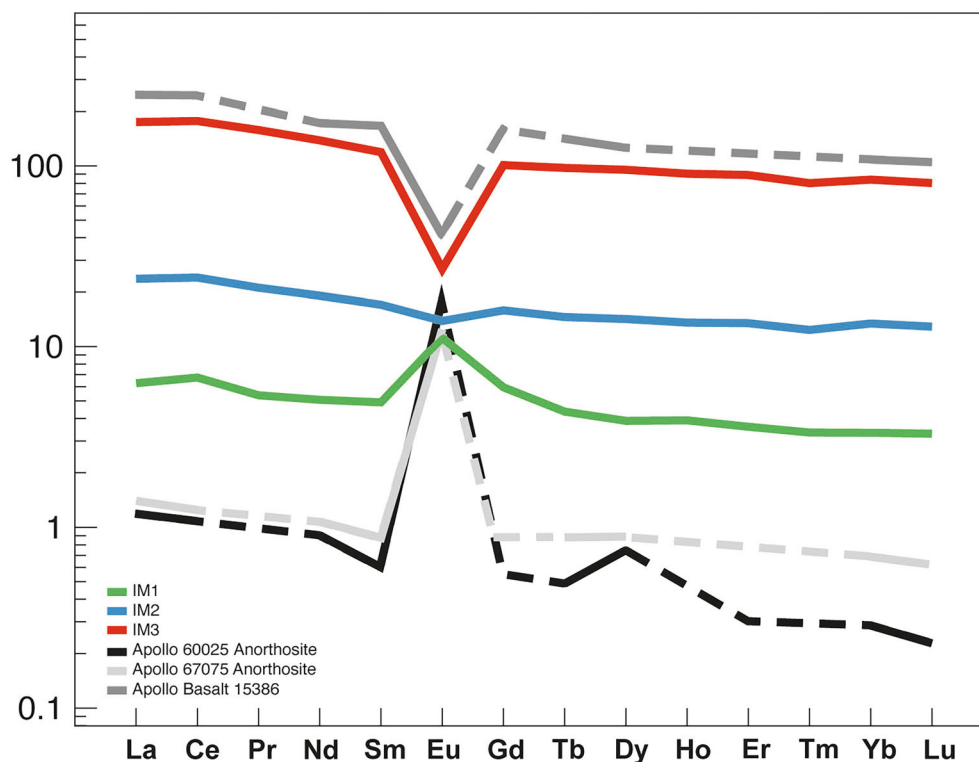


FIGURE 7. REE concentrations normalized to CI chondrites (Barrat et al., 2012) for the three impact melt lithologies (IM-1 to IM-3) from Dhofar 1769, in comparison with selected Apollo samples (Haskin et al., 1971, 1973, 1981; Warren & Wasson, 1978). IM-1 has a well-developed positive Eu anomaly related to low abundances of trivalent REE and a high anorthositic contribution, whereas the composition of IM-3 is similar to that of the KREEP basalt Apollo 15386 (Warren & Wasson, 1978). IM-2 has a relatively flat REE pattern. (Color figure can be viewed at wileyonlinelibrary.com)

Korotev (1996). The IMB from lunar meteorite NWA 7022 has a similar pattern with a pronounced negative Eu anomaly (Korotev, 1996), but the REE concentrations are lower by a factor of ~ 2 compared with those of IM-3 (Figure 9).

IM-2 is most similar to the group-3 melt rocks of Apollo 16, most of which are clast-poor and have subophitic–ophitic–intersertal textures (Korotev, 1994). Considering the REE abundances, the pattern for the IMB IM-2 is also very similar to that of the IMB within NWA 10783 (Korotev & Irving, 2021; Figure 9). The patterns are quite flat with a small enrichment of the light REE relative to the heavy ones, and they show a very weak negative Eu anomaly (especially in the case of IM-2).

IM-1 has a composition of the low-Al end of the range of “typical feldspathic highlands” as inferred from numerous feldspathic lunar meteorites (Korotev & Irving, 2021). Considering the REE pattern (Figure 9), IM-1 is similar to the fine-grained feldspathic microporphyritic melt breccias from Apollo 16 (63538, 67715, 67718, 67617; Stöffler et al., 1985). The REE composition of IM-1 is also almost indistinguishable

from the bulk rock of lunar meteorite Dhofar 081 (Warren et al., 2005). Dhofar 081 is one of many “typical feldspathic lunar meteorites” and overlaps in composition with the group-4 impact melt breccias of Apollo 16 (Korotev, 1994). As mentioned above, this rock has a high abundance of interstitial melt (Figure 8) and can be regarded as an IMB.

Formation of the Different Types of Impact Melts: How many Impact Events are Required?

IM-1: The first melt was produced in a highly anorthositic environment, as the bulk composition and the abundance of anorthite clearly point toward a highland location. The visible occurrence of many small Fe,Ni metal particles indicates a distinct contamination of the melt by the metal-bearing projectile. Considering an almost Ni-free anorthositic target highland rock and the ~ 100 ppm Ni and within the melt lithology, a contribution of about 1% of a chondritic projectile (~ 1.1 wt% Ni) during impact melt formation can be calculated. The contribution would be considerably less, if metal-rich projectiles were involved. However, as the

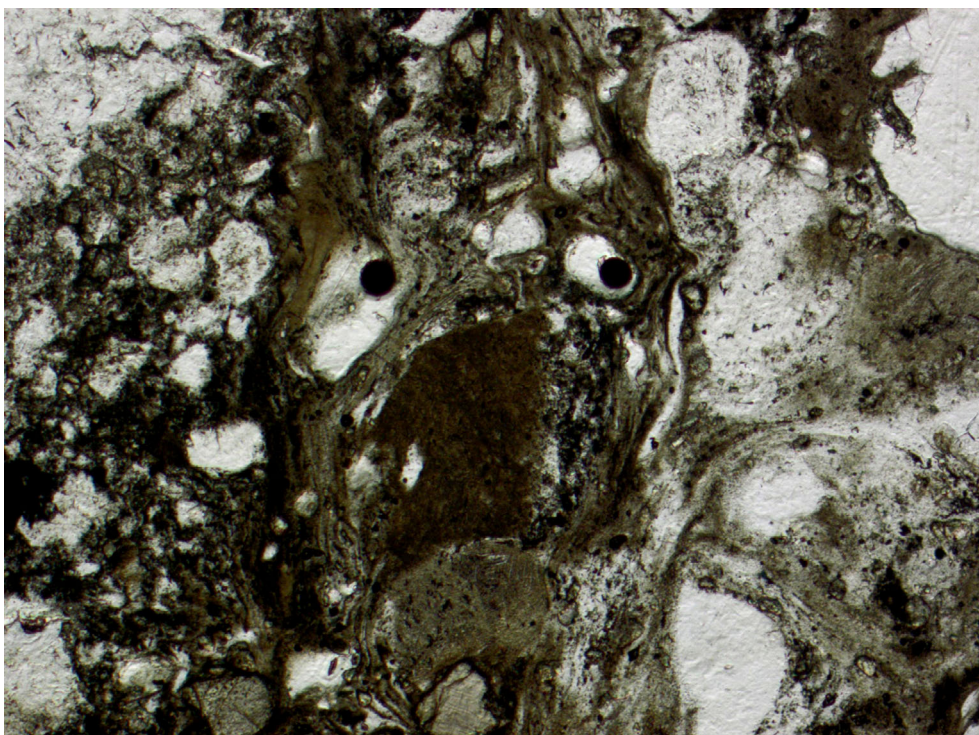


FIGURE 8. The entire bulk sample of Dhofar 081 can be regarded as an IMB. Light-colored fragments as well as gray-brownish clasts within the Dhofar 081 breccia are mostly surrounded by schlieren-textured melt produced during the lithification process, creating a feature we termed the “Crying Man in the Moon.” Width: ~1.4 mm. Image taken in plane-polarized light. (Color figure can be viewed at wileyonlinelibrary.com)

FeO concentration of IM-1 (2.55 wt%; Table 1) is low and the REE are about $10\times$ CI, an iron meteorite projectile can be generally ruled out. The REE enrichment (Figure 7) of about 5–10 times relative to the chondritic composition indicates the incorporation of another component, perhaps a basalt (compare Figure 7).

IM-2: The impact melt IM-1 is completely enclosed within the fine-grained microporphyritic impact melt IM-2. Considering the major element composition, this melt is also quite anorthositic (Table 1). The melt has slightly higher abundances of mafic minerals than determined for IM-1, which is also indicated by higher Fe and Mg concentrations compared with those in impact melt IM-1. Also, the REE show a relatively flat pattern, about 10–20 times enriched relative to IM-1 (Figure 7). The main component of IM-2 is certainly anorthositic in composition. However, a distinct amount of a mafic component with a negative Eu anomaly has to be included into the IM-2 melt in order to erase the strong positive Eu anomaly typical for anorthositic highland rocks.

IM-3: The combined IM-1 and IM-2 melt rocks occur as a small clast within the main melt lithology IM-3 (Figure 1). This melt rock is mafic and quite similar in bulk composition to that of a mare basalt (Figure 7). Thus, IM-3 formed by preferential impact melting of a

KREEP basalt-rich target, perhaps a regolith rich in basaltic clasts (~90%), with a low abundance of anorthositic rock clasts.

Considering the formation of Dhofar 1769, many impact events have to be considered that must have been experienced by the various components prior to entry into the Earth’s atmosphere:

1. IM-1 melt rock formation in a chemically highly anorthositic area (Figure 7).
2. Brecciation of the melt rock and transportation into a (nearby?) feldspar-rich regolith.
3. IM-2 formation in a plagioclase-rich environment and incorporation of IM-1 into the new melt.
4. Brecciation of the IM-2 melt breccia and transportation to a mafic-rich location.
5. IM-3 IMB formation in a mafic (KREEP-basaltic) environment (Figure 7).
6. Brecciation of the melt and transportation of the mafic-rich IM-3 melt breccia clast to the feldspathic source area of Dhofar 1769, since Dhofar 1769 is a highly feldspathic breccia (Korotev, 2023).
7. Lithification of Dhofar 1769 in the regolith environment, making a rock from regolith by shock (Bischoff, Rubin, et al., 1983; Kieffer, 1975).

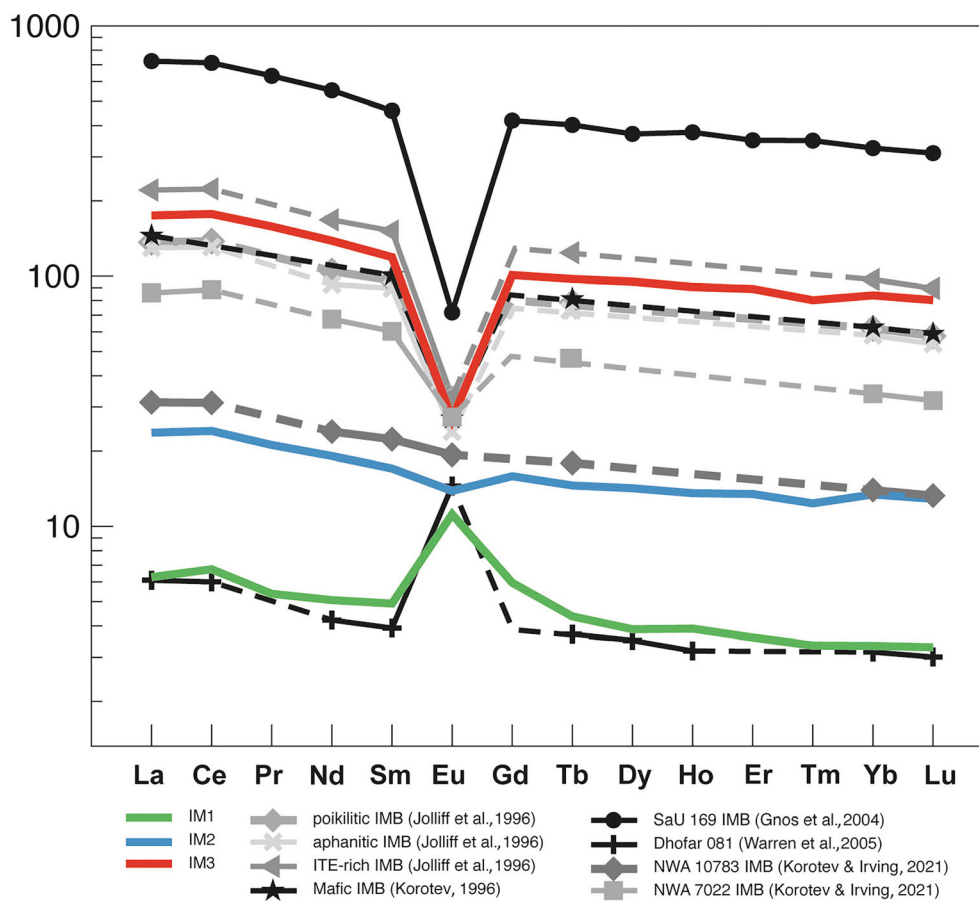


FIGURE 9. REE patterns of IM-1 to IM-3 in comparison with those of clasts from other lunar meteorites (Gnos et al., 2004; Korotev & Irving, 2021), Apollo 16 and 17 melt rock samples (Jolliff et al., 1996; Korotev, 1996), and bulk Dhofar 081 (Warren et al., 2005) that can be regarded as an impact melt breccia (IMB). From Apollo 17, mean compositions of particles from poikilitic IMBs, aphanitic IMBs, and incompatible trace element (ITE)-rich IMBs (Jolliff et al., 1996) are given. (Color figure can be viewed at wileyonlinelibrary.com)

8. Impact ejection of the brecciated Dhofar 1769 source rock from the Moon.
9. Impact with the Earth.

It cannot be ruled out that the lithification of the breccia and its ejection from the Moon happened in one single event. The impact on Earth led to a reduction of the mass of the traveling meteoroid. However, this certainly did not cause shock-induced modifications in the interior of Dhofar 1769.

The most unique characteristic of this breccia is the mixing of an anorthositic IMB within a mafic melt and the return of a fragment back into an anorthositic environment, where the host breccia of Dhofar 1769 was formed by shock lithification in the highland regolith.

CONCLUSIONS

Both sources of lunar materials (from space missions and meteorites) have the potential to provide important

information about surface processing on the Moon. Impact melt lithologies belong to the most abundant components in the lunar regolith and, thus, are important components to study in lunar regolith breccias.

In the case studied here, the chemical and mineralogical data clearly demonstrate the incorporation of a feldspar-rich subophitic crystalline melt within a feldspar-rich microporphyritic crystalline melt breccia, with this paragenesis itself having been embedded within a mafic crystalline melt breccia. Finally, the entire breccia with the three different impact melts must have been incorporated into the whole rock breccia. Consequently, considering the formation of the Dhofar 1769 source rock, many impact events have to be considered. For all processes of impact melt formations, additional steps of their brecciation, and relithification, a minimum number of seven impact processes is required. The most surprising event is the mixing of two anorthositic IMBs into a mafic melt and the return of a fragment back to an anorthositic environment, where the source breccia of Dhofar 1769

was formed by shock lithification in the highland regolith.

Acknowledgments—We thank U. Heitmann for sample preparation, Beate Schmitte for their analytical assistance, and Dr. Celeste Brennecka for editorial support. We greatly appreciate the valuable reviews of Randy Korotev and an anonymous reviewer as well as the scientific support and suggestions by the Associate Editor W.-U. Reimold and Mona Weyrauch. This work is partly funded by the Deutsche Forschungsgemeinschaft (DFG, German Research Foundation)—Project-ID 263649064—TRR 170 and TRR 170 publication no. 199. Open Access funding enabled and organized by Projekt DEAL.

Editorial Handling—Dr. Wolf Uwe Reimold

REFERENCES

- Barrat, J.-A., Zanda, B., Moynier, F., Bollinger, C., Liorzou, C., and Bayron, G. 2012. Geochemistry of CI Chondrites: Major and Trace Elements, and Cu and Zn Isotopes. *Geochimica et Cosmochimica Acta* 83: 79–92.
- Bischoff, A. 1996. Lunar Meteorite QUE93069: A Lunar Highland Regolith Breccia with Very Low Abundances of Mafic Components. *Meteoritics & Planetary Science* 31: 849–855.
- Bischoff, A. 2001. Fantastic New Chondrites, Achondrites, and Lunar Meteorites as the Result of Recent Meteorite Search Expeditions in Hot and Cold Deserts. *Earth, Moon & Planets* 85: 87–97.
- Bischoff, A., Palme, H., Spettel, B., Stöffler, D., Wänke, H., and Ostertag, R. 1986. Yamato 82192 and 82193: Two Other Meteorites of Lunar Origin. In *11th Symposium on Antarctic Meteorites*, 34–36. Tokyo: National Institute of Polar Research.
- Bischoff, A., Palme, H., Weber, H. W., Stöffler, D., Braun, O., Spettel, B., Begemann, F., Wänke, H., and Ostertag, R. 1987. Petrography, Shock History, Chemical Composition and Noble Gas Content of the Lunar Meteorites Y-82192 and Y-82193. *Memoirs National Institute of Polar Research* 46: 21–42.
- Bischoff, A., Rubin, A. E., Keil, K., and Stöffler, D. 1983. Lithification of Gas-Rich Chondrite Regolith Breccias by Grain Boundary and Localized Shock Melting. *Earth and Planetary Science Letters* 66: 1–10.
- Bischoff, A., Scott, E. R. D., Metzler, K., and Goodrich, C. A. 2006. Nature and Origins of Meteoritic Breccias. In *Book Chapter in "Meteorites and the Early Solar System II"*, edited by D. S. Lauretta, and H. Y. McSween, Jr., 679–712. Tucson, AZ: University of Arizona.
- Bischoff, A., and Stöffler, D. 1984. Clast Population Statistics of the Lunar Meteorite ALHA81005. *Lunar and Planetary Science* 15: 62–63.
- Bischoff, A., and Stöffler, D. 1985. Clast Population Statistics of the Lunar Meteorite Yamato 791197-Sample from a New Source Region of the Lunar Highlands? *Lunar and Planetary Science* 16: 63–64.
- Bischoff, A., and Stöffler, D. 1992. Shock Metamorphism as a Fundamental Process in the Evolution of Planetary Bodies: Information from Meteorites. *European Journal of Mineralogy* 4: 707–755.
- Bischoff, A., Stöffler, D., Borchardt, R., and Rehfeldt, A. 1983. Clast Population Statistics of Fragmental Breccias, North Ray Crater, Apollo 16: Implications for the Descartes Formation. *14th Lunar and Planetary Science Conference*, pp. 49–50.
- Bischoff, A., and Weber, D. 1997. Dar al Gani 262: The First Lunar Meteorite from the Sahara. *Meteoritics & Planetary Science* 32: A13–A14.
- Bischoff, A., Weber, D., Clayton, R. N., Faestermann, T., Franchi, I. A., Herpers, U., Knie, K., et al. 1998. Petrology, Chemistry, and Isotopic Compositions of the Lunar Highland Regolith Breccia Dar al Gani 262. *Meteoritics & Planetary Science* 33: 1243–57.
- Borchardt, R., Stöffler, D., Bischoff, A., and Reimold, W. U. 1983. Are the Descartes and Cayley Formations at Apollo 16 Characterized by Different Impact Melt Lithologies? *14th Lunar and Planetary Science Conference*, pp. 59–60.
- Bouvier, A., Gattacceca, J., Agee, C., Grossman, J., and Metzler, K. 2017. The Meteoritical Bulletin, No. 104. *Meteoritics & Planetary Science* 52: 2284.
- Day, J. M. D. 2020. Metal Grains in Lunar Rocks as Indicators of Igneous and Impact Processes. *Meteoritics & Planetary Science* 55: 1793–1807.
- Gnos, E., Hofmann, B. A., Al-Kathiri, A., Lorenzetti, S., Eugster, O., Whitehouse, M. J., Villa, I. M., et al. 2004. Pinpointing the Source of a Lunar Meteorite: Implications for the Evolution of the Moon. *Science* 305: 657–59.
- Haskin, L. A., Helmke, P. A., Allen, R. O., Anderson, M. R., Korotev, R. L., and Zweifel, K. A. 1971. Rare-Earth Elements in Apollo 12 Lunar Materials. *Proceedings of the Second Lunar Science Conference* 2: 1307–17.
- Haskin, L. A., Helmke, P. A., Blanchard, D. P., Jacobs, J. W., and Telander, K. 1973. Major and Trace Element Abundances in Samples from the Lunar Highlands *4th Lunar and Planetary Science Conference*, pp. 1275–96.
- Haskin, L. A., Lindstrom, M. M., Salpas, P. A., and Lindstrom, D. L. 1981. On Compositional Variations among Lunar Anorthosites *12th Lunar and Planetary Science Conference*, pp. 41–66.
- Jochum, K. P., Willbold, M., Raczek, I., Stoll, B., and Herwig, K. 2005. Chemical Characterization of the USGS, Reference Glasses GSA-1G, GSC-1G, GSD-1G, GSE-1G, BCR-2G, BHVO-2G and BIR-1G Using EPMA, ID-TIMS, ID-ICP-MS and LA-ICP-MS. *Geostandards and Geoanalytical Research* 29: 285–302.
- Jolliff, B. L., Korotev, R. L., and Haskin, L. A. 1991. Geochemistry of 2–4-mm Particles from Apollo 14 Soil (14161) and Implications Regarding Igneous Components and Soil-Forming Processes. *Proceedings of Lunar and Planetary Science* 21: 193–219.
- Jolliff, B. L., Rockow, K. M., Korotev, R. L., and Haskin, L. A. 1996. Lithologic Distribution and Geologic History of the Apollo 17 Site: The Record in Soils and Small Rock Particles from the Highland Massifs. *Meteoritics & Planetary Science* 31: 116–145.
- Joy, K. H., Crawford, I. A., Russell, S. S., and Kearsley, A. T. 2010. Lunar Meteorite Regolith Breccias: An In-Situ Study of Impact Melt Composition Using LA-ICP-MS with Implications for the Composition of the Lunar Crust. *Meteoritics & Planetary Science* 45: 917–946.
- Kieffer, S. W. 1975. From Regolith to Rock by Shock. *The Moon* 13: 301–320.

- Klemme, S., Prowatke, S., Münker, C., Magee, C., Lahaye, Y., Zack, T., Kasemann, S. A., Cabato, E. J. A., and Kaeser, B. 2008. Synthesis and Preliminary Characterisation of New Silicate, Phosphate and Titanite Reference Glasses. *Geostandards and Geoanalytical Research* 32: 39–54.
- Komnik, M. 2021. Dhofar 1769: Mineralogisch-Geochemische Untersuchungen an Lunaren Impaktschmelzen Bachelor Thesis, Institut für Planetologie, Westfälische Wilhelms-Universität Münster, 1–92.
- Korotev, R. L. 1987. The Meteorite Component of Apollo 16 Noritic Impact Melt Breccias. *Journal of Geophysical Research* 92: E491–E512. Proceedings of the 17th Lunar and Planetary Science Conference.
- Korotev, R. L. 1994. Compositional Variation in Apollo 16 Impact-Melt Breccias and Inferences for the Geology and Bombardment History of the Central Highlands of the Moon. *Geochimica et Cosmochimica Acta* 58: 3931–69.
- Korotev, R. L. 1996. On the Relationship between the Apollo 16 Ancient Regolith Breccias and Feldspathic Fragmental Breccias, and the Composition of the Prebasin Crust in the Central Highlands of the Moon. *Meteoritics & Planetary Science* 31: 403–412.
- Korotev, R. L. 2000. The great lunar hot spot and the composition and origin of the Apollo mafic (“LKFM”) impact-melt breccias. *Journal of Geophysical Research* 105: 4317–45.
- Korotev, R. L. 2023. Lunar Meteorites <https://sites.wustl.edu/meteoritesite/items/lunar-meteorites/>.
- Korotev, R. L., and Irving, A. J. 2021. Lunar Meteorites from Northern Africa. *Meteoritics & Planetary Science* 56: 206–240.
- Kuehner S. M., Irving A. J., and Korotev R. L. 2012. Petrology and Composition of Lunar Meteorite Northwest Africa 7022: An Unusually Sodic Anorthositic Gabbroic Impact Melt Breccia with Compositional Similarities to Miller Range 090036. *43rd Lunar and Planetary Science Conference*, abstract #1524.
- Ostertag, R., Stöffler, D., Bischoff, A., Palme, H., Schultz, L., Spettel, B., Weber, H., Weckwerth, G., and Wänke, H. 1986. Lunar Meteorite Yamato 791197: Petrography, Shock History and Chemical Composition. *Memiors of National Institute of Polar Research Special Issue* 41: 17–44.
- Palme, H., Spettel, B., Burghele, A., Dreibus, G., Weckwerth, G., Wänke, H., Jochum, K. P., Weber, H., Bischoff, A., and Stöffler, D. 1990. Big MAC, Little MAC and the Composition of the Lunar Crust. *Lunar and Planetary Science* 21: 930–31.
- Palme, H., Spettel, B., Jochum, K. H., Dreibus, G., Weber, H., Weckwerth, G., Wänke, H., Bischoff, A., and Stöffler, D. 1991. Lunar Highland Meteorites and the Composition of the Lunar Crust. *Geochimica et Cosmochimica Acta* 55: 3105–22.
- Reimold, W. U., and Borchardt, R. 1984. Subophitic Lithologies in KREEP-Rich Impact Melt Rocks from Cayley Plains, Apollo 16—Remnants of a Volcanic Highland Crust? *Earth and Planetary Science Letters* 67: 9–14.
- Ryder, G., and Ostertag, R. 1983. ALHA 81005: Moon, Mars, Petrography, and Giordano Bruno. *Geophysical Research Letters* 10: 791–94.
- Sokol, A. K., and Bischoff, A. 2005. Mineralogy of the Lunar Meteorites Kalahari 008 and Kalahari 009. *Meteoritics & Planetary Science* 40: A144.
- Sokol, A. K., Fernandez, V. A., Schulz, T., Bischoff, A., Burgess, R., Clayton, R. N., Münker, C., et al. 2008. Geochemistry, Petrology and Ages of the Lunar Meteorites Kalahari 008 and 009: New Constraints on Early Lunar Evolution. *Geochimica et Cosmochimica Acta* 72: 4845–73.
- Stelzner, T., Heide, K., Bischoff, A., Weber, D., Scherer, P., Schultz, L., Happel, M., et al. 1999. An Interdisciplinary Study of Weathering Effects in Ordinary Chondrites from the Afer Region, Algeria. *Meteoritics & Planetary Science* 34: 787–794.
- Stöffler, D., Bischoff, A., Borchardt, R., Burghele, A., Deutsch, A., Jessberger, E. K., Ostertag, R., et al. 1985. Composition and Evolution of the Lunar Crust in the Descartes Highlands, Apollo 16. *Journal of Geophysical Research* 90: C449–C506. 15th Lunar and Planetary Science Conference.
- Stöffler, D., Knöll, H.-D., Marvin, U. B., Simonds, C. H., and Warren, P. H. 1980. Recommended Classification and Nomenclature of Lunar Highland Rocks—A Committee Report. Proceedings Lunar and Planetary Institute Compiler Conference on the Lunar Highlands Crust, 51–70.
- Stöffler, D., Ostertag, R., Reimold, W. U., Borchardt, R., Malley, J., and Rehfeldt, A. 1981. Distribution and Provenance of Lunar Highland Rock Types at North Ray Crater, Apollo 16 *12th Lunar and Planetary Science*, pp. 185–207.
- The Meteoritical Bulletin. 2023. Accessed January 23, 2023. <https://www.lpi.usra.edu/meteor/about.php>
- Warren, P. H., Ulff-Møller, F., and Kallemeyn, G. W. 2005. “New” Lunar Meteorites: Impact Melt and Regolith Breccias and Large-Scale Heterogeneities of the Upper Lunar Crust. *Meteoritics & Planetary Science* 40: 989–1014.
- Warren, P. H., and Wasson, J. T. 1978. Compositional Petrographic Investigation of Pristine Nonmare Rocks. *9th Lunar and Planetary Science Conference*, pp. 185–217.
- Zipfel, J., Spettel, B., Palme, H., Wolf, D., Franchi, I., Pillinger, C. T., and Bischoff, A. 1998. Dar al Gani 400, Chemistry and Petrology of the Largest Lunar Meteorite. *Meteoritics & Planetary Science* 33: A171.

SUPPORTING INFORMATION

Additional supporting information may be found in the online version of this article.

Table S1a. Electron microprobe analyses (EMPA). Mineral compositions—plagioclase; n.d., not detected; all data in wt%.

Table S1b. EMPA mineral compositions—olivine; n.d., not detected; all data in wt%.

Table S1c. EMPA mineral compositions—pyroxene; n.d., not detected; all data in wt%.

Table S2. Chemical composition of metals in the studied impact melts IM-2 and IM-3 obtained by electron microprobe analysis; no large metal grain was found in IM-1; all data in wt%; n.d., not detected.

Figure S1. The large mafic crystalline impact melt breccia shown in Figure 1 encloses plagioclase-rich fragments (plag; black) as well as a crystalline feldspar-rich impact melt breccia as a fragment (indicated by the box). Note that the mafic lithology is characterized by a high abundance of pyroxenes (light gray) compared to the enclosed impact melt breccia containing abundant plagioclase. BSE image.
